ELSEVIER

GHGT-10

Numerical Modeling of CO_2 Mineralisation during Storage in Deep Saline Aquifers

Panneerselvam Ranganathan, Patrick van Hemert, E. Susanne J. Rudolph, Pacelli Z.J. Zitha[*]

Department of Geotechnology, Delft University of Technology, Stevinweg 1, 2628CN Delft, The Netherlands

Abstract

Simulations are performed to evaluate the feasibility of a potential site within the Rotliegend sandstone formation in the Dutch subsurface at a depth of around 3000 m for CO_2 sequestration using the numerical simulator CMG-GEM. Three CO_2 storage trapping mechanisms are studied: (1) mobility trapping, (2) solubility trapping, and (3) mineral trapping. Results show that the injected CO_2 initially migrates towards the top of the reservoir due to gravity segregation. Then the CO_2 spreads laterally and dissolves in the formation water (brine). Due to the dissolution of CO_2 the density of the brine increases, which then results in fingering due to gravity. Further, the effect of mineralisation is included in the simulation. It is found in this study that considerable amounts of CO_2 are stored mainly by solubility and mobile trapping. The contribution of mineral trapping is insignificant. Additionally, the effect of varying the permeability and the residual gas saturation on the CO_2 storage-capacities are studied. It is found that a random permeability field enhances CO_2 capturing by means of solubility trapping, while a higher residual gas saturation enhances the CO_2 storage by means of mobility trapping.

1. Introduction

Storage of CO_2 in deep saline aquifers is one way to reduce the increasing greenhouse gases in the atmosphere. Large-scale injection of CO_2 into saline aquifers involves a variety of coupled physical and chemical processes including multiphase fluid flows, solute transport, and chemical reactions between fluids and formation minerals. A part of the injected CO_2 dissolves in the brine, forms carbonic acid and decomposes into H^+ and HCO_3^- ions decreasing the pH of the brine. The dissolved ions present in the aqueous phase react with minerals of the formation. Eventually, the above mentioned geochemical reactions result either in precipitation or dissolution of minerals, newly formed or originally present,

———————

[*] Corresponding author. Tel.: +31 (0) 15 27 88437, Fax: +31 (0) 15 27 81189.
 E-mail address: P.L.J.Zitha@tudelft.nl

changing the porosity and the permeability of the matrix. This governs the long-term fate of injected CO_2. It is critically important therefore to understand and investigate the CO_2 mineralisation process during CO_2 storage in saline aquifers using a simulator which also accounts for the occurring geochemical processes. Various research groups [1, 2] performed reactive transport simulations to study the impact of different parameters such as kinetic rate constants and reactivity on geological sequestration of CO_2. Also, some studies [3, 4] have been done examining the storage capability of specific sites (large scale and pilot scale).

In this work, CO_2 mineralisation, accompanying CO_2 storage in deep saline aquifers in a Rotliegend sandstone formation, is studied using the commercial simulator CMG-GEM. CMG-GEM is a reactive transport module capable of handling CO_2 sequestration in aquifers simultaneously accounting for geochemical reactions. The Rotliegend sandstone formation as commonly found in the Dutch subsurface, is regarded as a suitable location for CO_2 storage. Its estimated storage capacity is 337 Mtons [5]. Rotliegend sandstones of the Slochteren formation are found at various locations in the Netherlands, namely in northern Noord-Holland, in Friesland, Drenthe and Groningen. The objective of the present work is to carry out a feasibility study of CO_2 storage by means of mineralisation with a simulation time of 10,000 years. For the simulation it is assumed to inject yearly 1.0 MTones of CO_2 in the first 16 years. Common input parameters for the simulations are the (relative) permeability, or the way how the permeability is described, and the residual gas saturation. Therefore, it is crucial to know what the impact of changing permeability or residual gas saturation is on the simulation results. Therefore, a sensitivity study is carried out.

2. Hydrogeological Model

The Rotliegend sandstone formation is group of the lower Permian. This formation is considered suitable for CO_2 storage. The Rotliegend Sandstone formation meets the general criteria for CO_2 storage in aquifers as outlined by van der Meer and Yavuz, [5]. It lies at depths greater than 800 m. Its overburden layer is the permain Zechstein salt which acts as impermeable caprock and has an average thickness of 50 m and depth of around 3000-4500 m.

A three dimensional Cartesian geological model of 15 km×15 km×50 m, distributed into ten layers by grid blocks of 300 m x 300m x 5m, is used to study the spatial distribution and temporal evolution of injected CO_2 and the subsequent changes due to spreading of the CO_2 and the occurring geochemical reactions. The injection well is located at the centre of the model. CO_2 is injected over the total length of the well using a constant rate of 1.0MTon /year for the period of 16 years. The constant pressure boundary is specified at the outer grid elements to have an open boundary with a large part of the aquifer outside of the computational domain. The simulation is carried out to study fluid flow through porous media and geochemical transport over a period of 10,000 years

The input parameters for the simulations are given in Table 1. The formation is considered homogeneous with an average porosity and permeability of 0.18 and 200mD respectively. The water and gas relative permeability curves are obtained using the Brooks-Corey equation:

$$k_{rw} = k_{rw}^{\circ} \left(\frac{S_w - S_{wr}}{1 - S_{wr}} \right)^{N_w} \qquad \text{.............(1)}$$

$$k_{rg} = \left(1 - \hat{S} \right)^2 \left(1 - \hat{S}^2 \right) \quad \text{where} \quad \hat{S} = \frac{(1 - S_{lr})}{(1 - S_{lr} - S_{gr})} \qquad \text{.............(2)}$$

where S_{wr} is the irreducible water saturation, S_{gr} is the irreducible gas saturation, N_w is the water relative permeability exponent, and k_{rw} is the water end point relative permeability,
The capillary pressure curve is computed by van Genuchten, [6]

$$P_{cap} = -P_0 \left(\left[S^* \right]^{-1/m} - 1 \right)^{-1/m} \qquad \text{.............(3)}$$

where $S^* = \left(\frac{S_l - S_{lr}}{1 - S_{lr} - S_{gr}} \right)$ with $S_{lr} = 0.0$, m = 0.425, and P_0 = 19.61 kPa

Table 1: Hydrogeological parameters used in the study

Parameters	Rotliegend (sandstone) formation
length (km)	15
width (km)	15
thickness (m)	50
grid	50×50×10
depth of top of reservoir (m)	3000
porosity	0.18
horizontal permeability (mD), k_h	200
vertical permeability (mD), k_v	0.1 x k_h
initial reservoir temperature (C)	50
initial reservoir pressure (MPa)	28
salinity of formation water (PPM)	100,000

Relative permeability	
residual water saturation	0.2
water end point relative permeability	1.6
water permeability exponent	3.0
residual gas saturation	0.05, 0.2
Injectivity	
injection rate	1 Mton/year for first 16 years
simulation period	10,000 years

The Rotliegend sandstone consists mainly of quartz. Other minerals such as K-feldspar, dolomite, kaolinite and Illite occur only in minor amounts [7]. Unfortunately, for the Rotliegende sandstone formation of interest, there are no accurate data on the mineral composition and on the composition of the formation water. Instead the mineral composition and data on the formation water chemistry are taken from reported data on Rotliegend sandstone formation of the UK [8]. This approach is justified due to the fact that the Rotliegend sandstone formation in the Netherlands and the Rotliegend sandstone formation of the southern part of the UK are connected and comparable. In Table 2 the composition of the formation is given, in Table 3 the composition of the formation water. The geochemical reactions considered in the simulations and their reaction kinetic paramaters are given in Table 4. The reaction kinetic parameters are taken from literature [9].

Table 2: Mineral Composition of Rotliegend sandstone formation (Wilkinson et al. [8])

Sandstone Mineral compositions	Volume fraction
Quartz	0.51
Rock fragments	0.12
K-Feldspar	0.07
Plagioclase	0.0
Dolomite	0.14
Kaolinite	0.03
Illite	0.006

Table 3: Composition of Rotliegend sandstone formation

Aqueous species	Molality (mol /kg of water)
H^+	1.642E-08
Fe^{2+}	6.116E-03
Ca^{2+}	1.609E-01
SiO_2	8.642E-04
Al^{3+}	5.573E-07
K^+	5.097E-01
Mg^{2+}	3.443E-02
OH^-	5.662E-05
HCO_3^-	1.440E-02
CO_3^{2-}	1.467E-07

Table 4: Main reactions used in simulation (Kinetic parameters are from Nghiem et al. [9])

Aqueous Reactions	Log Keq (Nghiem et al. [9])		
$H_2O \leftrightarrow H^+ + OH^-$ $CO_{2(aq)} + H_2O_{(l)} \leftrightarrow HCO_3^-{}_{(aq)} + H^+{}_{(aq)}$ $HCO_3^-{}_{(aq)} \leftrightarrow CO_3^{2-}{}_{(aq)} + H^+{}_{(aq)}$	-13.2631 -6.3221 -16.5563		
Mineral Reactions	**Log Keq**	**Reactive surface area (m²/m³)**	**Rate constant**
Quartz $\leftrightarrow SiO_2(aq)$	-3.629	7128	-13.90
Kaolinite + $6H^+ \leftrightarrow 5H_2O + 2Al^{3+} + 2\ SiO_2(aq)$	5.4706	17600	-12.00
Dolomite + $2H^+ \leftrightarrow Ca^{2+} + Mg^{2+} + 2\ HCO_3^-$	1.6727	88	-9.222
K-Feldspar + $4H^+ \leftrightarrow 2H_2O + K^+ + Al^{2+} + 3SiO_2(aq)$	-0.344	176	-13.00
Illite + $8H^+ \leftrightarrow 0.6K^+ + 0.25Mg^{2+} + 2.3\ Al^{3+} + 3.5SiO_2(aq) + 5H_2O$	7.4855	26400	-14.00

3. Numerical Methods

The simulations are performed using the commercial compositional Generalised Equation of State simulator (CMG-GEM). The governing equations are given below [9]

For the components of the gaseous phase (g) the mass balance equation is given by:

$$\frac{\partial N_{ig}}{\partial t} = \nabla \cdot \left(\frac{\rho_g kk_{rg} m_{ig,g}}{\mu_g} \right)(\nabla p + \nabla p_{cwg} - \rho_g g \nabla z) + \nabla \cdot \left(\frac{\rho_w kk_{rw} m_{ig,w}}{\mu_w} \right)(\nabla p + \nabla p_{cwg} - \rho_w g \nabla z) + \nabla \cdot J_{ig} + \sigma_{ig,aq} + q$$

……………….(4)

For the components in the aqueous phase (aq)

$$\frac{\partial N_{ia}}{\partial t} = \nabla \cdot \left(\frac{\rho_w kk_{rw} m_{ia,w}}{\mu_w} \right)(\nabla p - \rho_w g \nabla z) + \nabla \cdot J_{ia} + \sigma_{ia,aq} + \sigma_{ia,mn} + q$$

……………..(5)

For the minerals (m)

$$\frac{\partial N_{km}}{\partial t} = \sigma_{km,mn}$$

……………..(6)

where J_{ig} is diffusion / dispersion of gas component, J_{ja} is diffusion/dispersion of aqueous component , N_{ig} is the number of moles of gas component i per grid volume, N_{ja} is the number of moles of aqueous component i per grid volume, N_{km} is the number of moles of minerals per grid volume, $m_{ig,g}$ is the mole fractions of gas component i in gas phase, $m_{ig,w}$ is the mole fractions of gas component i in aqueous phase, $m_{ja,w}$ is mole fraction of aqueous component i in aqueous phase , $\sigma_{ig,aq}$ is reaction rate between gaseous and aqueous component, $\sigma_{ia,aq}$ is reaction rate between aqueous and aqueous component, $\sigma_{ia,mn}$ is reaction rate between aqueous and mineral component, q is well molar flow rate of gas component, $\sigma_{km,mn}$ is mineral reaction rate, ρ_g is density of gas, ρ_w is density of water, P is water pressure, P_{cwg} is capillary pressure between water and gas, g is gravity, k is permeability, k_{rg} is gas relative permeability, k_{rw} is water relative permeability, t is time step, and Z is depth,

The first terms at left hand side of equations (4) (5) & (6) represent the accumulation. The first and second terms at the right hand side of equations (4), and (5) describe convective and diffusive transport respectively. q in equations (4) & (5) are the flow rates and , in this study, represent the CO_2 injection rate. The mineral dissolution/precipitation due to chemical reactions with the components forming the aqueous phase ($\sigma_{km,mn}$) in equations (6) are governed by the following equations

$$R_i = \hat{A}_i k_i \left[1 - \frac{Q_i}{K_{eq,i}} \right]$$

……………..(7)

where $\hat{A}_i$ is reactive surface area for mineral i, k_i is reaction rate constant, Q_i is activity product of mineral reaction i, and $K_{eq,i}$ is the equilibrium constant for mineral reaction.

The numerical method which is adopted for solving the above governing equations is based on the finite difference method [9]. Further, the adaptive-implicit discretisation is used. Newton's method is used to simultaneously solve the equations describing the flow, the phase equilibrium, the chemical equilibrium and the mineral dissolution and precipitation rates. The Jacobian matrix in Newton's method is a sparse matrix that is solved by Incomplete LU (ILU) factorization followed by the GMRES iterative method [9].

4. Results and Discussion

4.1 Base case simulation

Figure 1 and 2 show the spatial distribution of CO_2 (gas) saturation and CO_2 dissolved in the aqueous phase in terms of mole fractions at various simulation times: (a) after 16 years (shut-in), (b) after 5,000 years and (c) after 10,000 years. The figures show the 3D model cut-off in y-direction at J=25, the injection plane, in order to obtain clear profiles which allow analysis of the results. It is shown that a gas plume is formed which increases in extension towards the top of the reservoir. This is due to the density differences between the aqueous phase and the supercritical CO_2 (see Figure 1a). This is called mobility trapping. Only small amounts of supercritical CO_2 are trapped in the porous rock as residual gas after it has migrated towards the top of the reservoir. After the injection period, when no further CO_2 is added to the reservoir, CO_2 present in the reservoir moves upwards and laterally accumulates in the top layer (see Figure 1b). The horizontal movement of the CO_2 is faster than the vertical movement of the gas (k_v=0.1 k_h) so that a mushroom-like distribution of the gas is observed (see Figure 1c). As can be seen from Figure 2 the supercritical CO_2 does not only flow upwards in the reservoir due to gravity differences but also dissolves in the water. The mass transfer of CO_2 into the aqueous phase is slower than the movement of the supercritical gas through the reservoir. Consequently, the highest concentrations of dissolved CO_2 are observed close to the injection well and in the upper layers of the reservoir, comparable to the distribution of supercritical gas in the reservoir. Due to gravity effects and concentration gradients the CO_2 further dissolves in the aqueous phase which results in the observed fingering from the upper layer towards the lower layers (see Figure 2b and 2c).
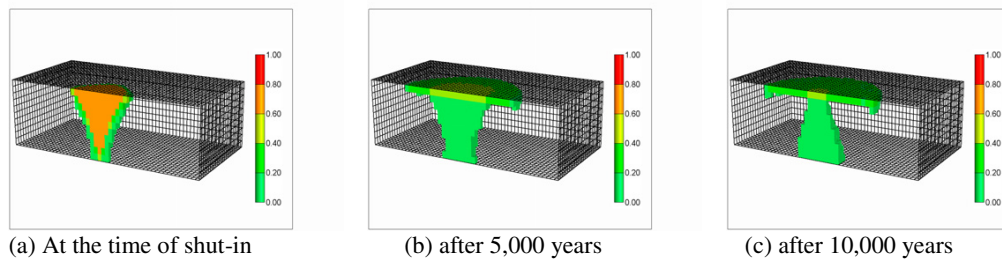
(a) At the time of shut-in	(b) after 5,000 years	(c) after 10,000 years

Figure 1: Base case without mineralisation: spatial distribution of CO_2 (gas) saturation at various simulation times.

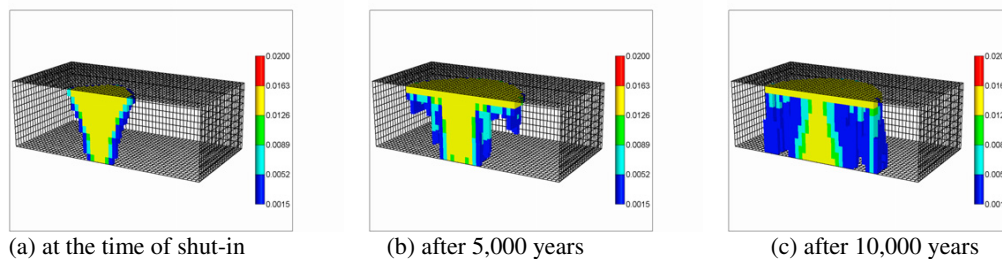| (a) at the time of shut-in	(b) after 5,000 years	(c) after 10,000 years

Figure 2: Base case without mineralisation: spatial distribution of CO_2 dissolved in the aqueous phase at various simulation times given in terms of mole fractions.

4.2 Effect of Mineralisation

Figure 3 shows the spatial distributions of CO_2 gas saturation, dissolved CO_2 and of the concentration of several minerals (feldspar, quartz, dolomite, kaolinite) after a simulation time of 10,000 years. The change of number of moles of several minerals with time is shown in Figure 4. Analysing the simulation results allow the following conclusions. Just as for the base case simulations it is observed that gaseous CO_2 migrates upward and accumulates in the top layer beneath the sealing cap rock (Figure 3a) and that the front of CO_2 dissolved in brine moves from the top layer downwards (Figure 3b). From Figure 3c and 3e it can be concluded that injected CO_2 is converted into kaolinite and to a smaller extent into dolomite which then precipitates (Fig. 3c, e). In order for kaolinite to precipitate aluminium needs to be present. This is provided by dissolution of alumosilicates like feldspar (see Figure 3d). The formation of kaolinite in Rotliegend sandstones has already been observed by others [7]. Precipitation of dolomite (see Figure 3c) requires the presence of clay minerals of divalent cations such as Ca^{2+}, Mg^{2+}, and Fe^{2+} which are generally released from the dissolution of primary minerals. In Rotliegend sandstone formations the amount of released divalent cations by dissolution of primary minerals is very small due to lack of available cations. Consequently, smaller amounts of dolomite precipitate (see also Figure 3c, 3e and 3f).

In section 3 the reaction schemes describing the dissolution of CO_2 in the aqueous phase, and the dissolution and the precipitation of various minerals are given. From these it can be concluded that in order to sequestrate CO_2 by means of mineralisation it is important to dissolve CO_2 to form HCO_3^- but also to dissolve quartz (see chemical reactions section 3). Only if sufficient HCO_3^- ions and $SiO_2(aq)$ are present CO_2 can be successfully stored as dolomite, kaolinite or illite. Analysing the simulation results (Figure 3 and 4) it can be seen that only kaolinite clearly increases with time while dolomite slightly increases and illite even decreases strongly with time. At the same time the quartz concentration increases in the same manner as kaolinite (see Figure 4). This is an indication that CO_2 sequestration in a saline aquifer by means of mineralisation is limited.
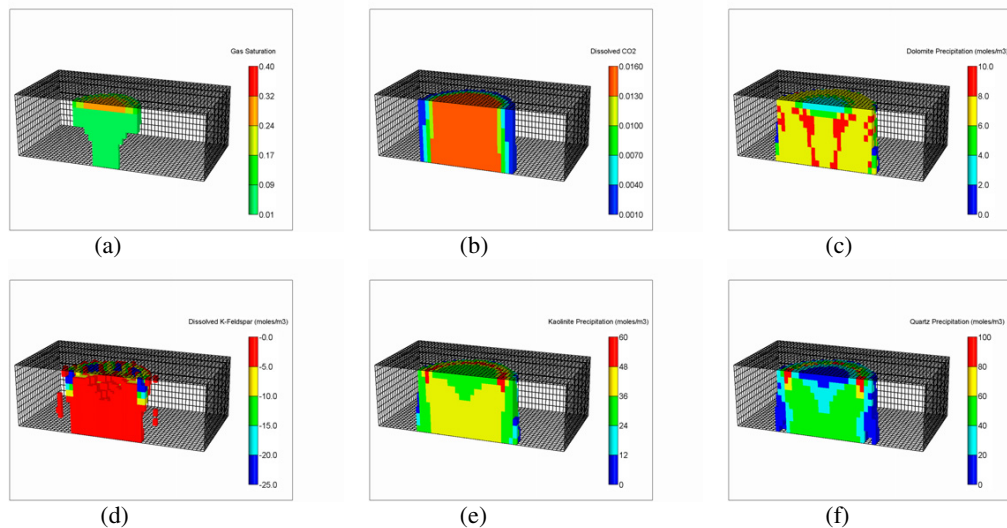

Figure 3: Base case with mineralisation: spatial distribution of various components after simulation time of 10,000 years (a) CO_2 gas saturation and (b) concentration of dissolved CO_2 (c) Quartz fraction (d) Kaolinite fraction (e) K-Feldspar fraction (f) Dolomite fraction.

There are basically three main trapping mechanisms which are responsible for CO_2 storage in a saline aquifer, i.e., mobility trapping, solubility trapping and mineral trapping. In Figure 5 the amount of CO_2 stored by each mechanism as function of time is shown. During the injection period (first 16 years of the simulation), mobility trapping dominates contributing up to 90% whereas solubility trapping contributes only around 10 %. Mineral trapping is not occurring in the first few years. Only after around 200 years the

amount of CO_2 captured by mineralisation slowly increases. With increasing time, solubility and mineral trapping increase gradually while mobility trapping decreases. After 10,000 years, approximately 60 % of CO_2 injected is trapped by solubility trapping, about 30 % is trapped by mobility trapping and only 10 % by mineralisation. Thus, it can be concluded from the present study that in Rotliegend sandstone reservoirs the most CO_2 is stored by solubility and mobility trapping while mineral trapping plays an insignificant role.
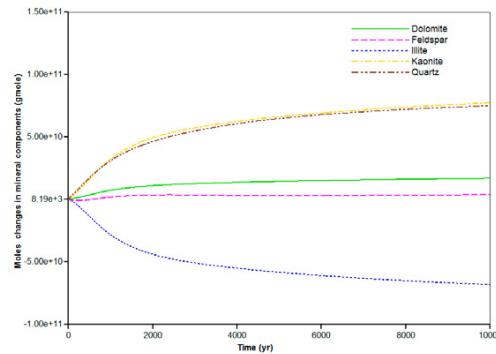

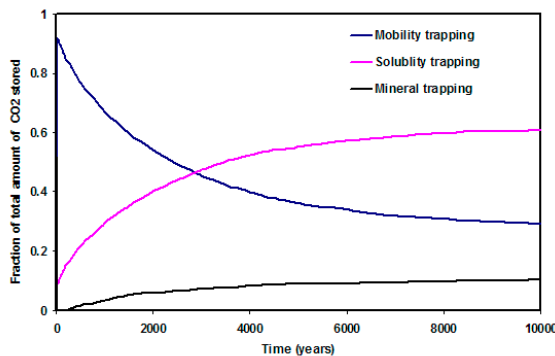Figure 4: Base case with mineralsiation: changes of number of moles of minerals as function of time

Figure 5: Base case with mineralisation: Fractions of total amount of captured CO_2 by each trapping mechanism
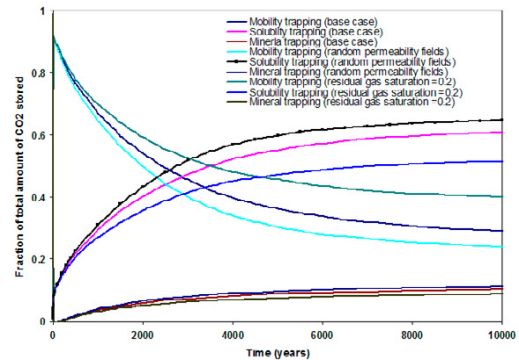

Figure 6: Sensitivity analysis on fraction of total amount of CO_2 stored by each trapping mechanism

4.3 Sensitivity analysis

In Figure 6 the effect of changing the permeability field and of assuming a higher residual gas saturation on the CO_2 storage is shown. The importance of these hydrogeological parameter on CO_2 storage are also reported in literature [2, 10]. The permeability field was changed from a layered but homogenous reservoir into a reservoir with a stochastically generated permeability field with a mean permeability of 200 mD, a correlation length of 300 m in both x and y-directions and of 5 m in z-direction and a Dykstra-Parson coefficient of 0.7. The influence of the residual gas saturation was investigated by increasing the residual gas saturation from 0.05 (base case) to 0.20.

From Figure 6 it can be concluded that in a randomly distributed permeability field with the same mean permeability as in the base case the trapping of CO_2 by means of mineralisation and solubility is enhanced. At the contrary a higher residual gas saturation enhances the CO_2 capture by means of mobility trapping. Thereby, for both cases the influence on the mineralisation trapping is the least and almost negligible. The improved capture by means of solubility trapping in the case of a stochastically generated permeability field may be due to a slower upward migration of the injected CO_2 to the top of the formation so that more CO_2 can dissolve in the formation water. The improved trapping of CO_2 by means of mobility

trapping as observed for a higher residual gas saturation, is due to the higher relative permeability to gas because of the higher gas saturation in the reservoir. Consequently, CO_2 can more easily move up in the reservoir and the dissolution of CO_2 into the aqueous phase decreases. This result is consistent with results found in literature [2].

5. Conclusions

The results of numerical simulations describing CO_2 sequestration in a Rotliegend sandstone formation are presented. In these simulations the occurring geochemical reactions are accounted for. The results show that injected CO_2 initially migrates towards the top of the reservoir due to gravity segregation. Then, CO_2 spreads laterally and dissolves in the formation water. The dissolution of CO_2 results in an increase of the density of the brine, which causes fingering due to gravity. During the CO_2 injection period, most of CO_2 is trapped by so-called mobility trapping while solubility trapping contributes only slightly and mineral trapping is not observed. With increasing time, capturing of CO_2 by mobile trapping decreases, while CO_2 storage by solubility trapping increases. Even though, CO_2 storage by mineral trapping increases gradually with time, its contribution is always clearly the smallest. It can be concluded that most of the CO_2 is stored by solubility and mobility trapping. For the sensitivity study, the effect of permeability variation and residual gas saturation on the storage of CO_2 are studied. Hardly any changes in the trapping of CO_2 by means of mineralisation were observed. A random permeability field enhances CO_2 capturing by means of solubility trapping, while a higher residual gas saturation enhances the CO_2 storage by means of mobility trapping.

The mineral trapping of CO_2 in Rotliegend sandstone reservoirs may be higher for other compositions of primary minerals, mineral reaction rates (kinetic rate constant and reactive surface area) and hydrogeological parameters (rock-fluid-CO_2). Thus, the examination of these uncertainties are needed. Further, because of the importance of the reactivity of the storage reservoir the feedback calculation of changes in permeability due to precipitation and dissolution of minerals should be investigated in future.

6. Acknowledgements

7. References

[1] Xu T, Apps JA, Pruess K. Numerical simulation of CO_2 disposal by mineral trapping in deep aquifers. Appl Geochem 2004: 19: 917-936.

[2] Audigane P, Gaus I, Czernichowski-Lauriol I, Pruess K, Xu T. Two-Dimensional Reactive Transport Modeling of CO_2 Injection in a Saline Aquifer at the Sleipner Site. Am J Sci 2007; 307: 974-1008.

[3] Hovorka SD, Doughty C, Holtz M. Testing efficiency of storage in the subsurface: Frio brine pilot experiment. Lawrence Berkeley Natl Lab Rep LBNL-55730; 2004

[4] Gaus I, Azaroual M, Czernichowski-Lauriol I. Reactive transport modeling of the impact of CO_2 injection on the clay cap rock at Sleipner (North Sea). Chem Geol 2005; 217: 319-337.

[5] van der Meer LGH (Bert), Yavuz Ferhat. CO_2 storage capacity calculations for the Dutch subsurface, Energy Procedia 2009; 1: 2615-2622

[6] Van Genuchten MT, A closed-form equation for predicting the hydraulic conductivity of unsaturated soils, Soil Sci Soc Am J 1980; 44: 892-898.

[7] Ziegler K. Clay minerals of the Permian Rotielgend group in the North Sea and adjacent areas. Clay Minerals 2006, 41 355–393.

[8] Wilkinson M, Stuart Haszeldine R, Fallick AE, Odling N, Stoker SJ. Gatliff, RW. CO_2–mineral reaction in a natural analogue for CO_2 storage-implications for modeling. J Sedimentary Res 2009, 79: 486–494.

[9] Nghiem L, Sammon P, Grabenstetter J, Ohkuma H. Modeling CO_2 storage in aquifers with a fully coupled geochemical EOS compositional simulator. SPE Paper No 89474; 2004.

[10] Kumar A, Ozah R, Noh M, Pope GA, Bryant S, Sepehrnoori K, Lake LW. Reservoir simulation of CO_2 storage in deep saline aquifers. SPE Paper No 89343; 2005.